OXFORD

Human Molecular Genetics, 2019, Vol. 28, No. 2 279–289

doi: 10.1093/hmg/ddy349
Advance Access Publication Date: 5 October 2018
General Article

GENERAL ARTICLE

Dusp6 is a genetic modifier of growth through enhanced ERK activity

Andy H. Vo[1], Kayleigh A. Swaggart[2], Anna Woo[3], Quan Q. Gao[3], Alexis R. Demonbreun[3], Katherine S. Fallon[3], Mattia Quattrocelli[3], Michele Hadhazy[3], Patrick G.T. Page[3], Zugen Chen[4], Ascia Eskin[4], Kevin Squire[4], Stanley F. Nelson[4] and Elizabeth M. McNally[3,*]

[1]Committee on Development, Regeneration and Stem Cell Biology, The University of Chicago, Chicago, IL 60637, [2]Department of Human Genetics, The University of Chicago, Chicago IL 60637, [3]Center for Genetic Medicine, Northwestern University Feinberg School of Medicine, Chicago IL 60611 and [4]Departments of Human Genetics and Pathology and Laboratory Medicine, David Geffen School of Medicine, University of California Los Angeles, Los Angeles, CA 90095, USA

*To whom correspondence should be addressed at: Center for Genetic Medicine, Lurie Research Building, 7-127 303 E. Superior St, Chicago, IL 60611, USA. Tel: +312 5035600; Fax: +312 5036210; Email: Elizabeth.mcnally@northwestern.edu

Abstract

Like other single-gene disorders, muscular dystrophy displays a range of phenotypic heterogeneity even with the same primary mutation. Identifying genetic modifiers capable of altering the course of muscular dystrophy is one approach to deciphering gene–gene interactions that can be exploited for therapy development. To this end, we used an intercross strategy in mice to map modifiers of muscular dystrophy. We interrogated genes of interest in an interval on mouse chromosome 10 associated with body mass in muscular dystrophy as skeletal muscle contributes significantly to total body mass. Using whole-genome sequencing of the two parental mouse strains combined with deep RNA sequencing, we identified the Met62Ile substitution in the dual-specificity phosphatase 6 (*Dusp6*) gene from the DBA/2 J (D2) mouse strain. DUSP6 is a broadly expressed dual-specificity phosphatase protein, which binds and dephosphorylates extracellular-signal-regulated kinase (ERK), leading to decreased ERK activity. We found that the Met62Ile substitution reduced the interaction between DUSP6 and ERK resulting in increased ERK phosphorylation and ERK activity. In dystrophic muscle, DUSP6 Met62Ile is strongly upregulated to counteract its reduced activity. We found that myoblasts from the D2 background were insensitive to a specific small molecule inhibitor of DUSP6, while myoblasts expressing the canonical DUSP6 displayed enhanced proliferation after exposure to DUSP6 inhibition. These data identify DUSP6 as an important regulator of ERK activity in the setting of muscle growth and muscular dystrophy.

Introduction

Muscular dystrophies, like most Mendelian disorders, arise from mutations in single genes that associate with variable penetrance and expressivity. In addition to environmental effects, genetic factors contribute to phenotypic variability, and discovering genetic modifiers for single gene disorders defines pathways that may be exploited for prognostic and therapeutic

Received: June 11, 2018. **Revised:** August 16, 2018. **Accepted:** September 26, 2018

purposes. Mutations within the genes encoding the dystrophin glycoprotein complex cause muscular dystrophy and genetic modifiers have been identified that influence these forms of muscular dystrophy (1–3). Limb-girdle muscular dystrophy type 2C (LGMD 2C) arises from mutations that disrupt the γ-sarcoglycan (SGCG) gene. SGCG is a dystrophin associated protein and its null mutations lead to a similar phenotype as dystrophin mutations in Duchenne muscular dystrophy (DMD) (4,5), although considerable phenotypic variability is present even with the same single primary SGCG mutation (5). Thus, additional factors influence disease outcomes in muscular dystrophy.

To identify genetic modifiers, quantitative trait locus (QTL) mapping has been applied to the *Sgcg* mouse model of LGMD2C (6–8). *Sgcg* mice were generated by deleting exon 2, which creates a null mutation, and like their human counterparts with LGMD 2C, *Sgcg* mice have muscle membrane disruption, loss of myofibers, extensive muscle fibrosis and accompanying cardiomyopathy (9). A backcross strategy was used to show that genetic background strains in mice confer mild and severe phenotypes to the *Sgcg* mouse (6). The DBA/2J (D2) strain exacerbates features of muscular dystrophy in mice and this has been shown for both *Sgcg* mice as well as *mdx* mice, the model for DMD (6,10,11). In the D2 strain, muscular dystrophy models have more muscle weakness, increased muscle fibrosis and greater Evans blue-dye uptake, a marker of muscle membrane fragility (10,12). The D2 strain is also associated with impaired muscle regeneration in muscular dystrophy (10,11). Diminished muscle regeneration, in concert with the progressive degeneration in muscular dystrophy, is thought to contribute to the overall smaller muscle size in muscular dystrophy in the D2 strain (6). This is in contrast to what is observed in wild-type (WT) non-dystrophic mice, where the D2 strain is larger (13).

Using an intercross of *Sgcg*-null mice from the severe D2 and mild 129 background strains (8), two different modifiers have been identified for muscular dystrophy (7,14). The first modifier discovered through this approach was *Ltbp4* (7). A 36 bp in-frame deletion was identified in *Ltbp4* from the D2 background. *Ltbp4* encodes latent TGFβ binding protein 4 (LTBP4) and the 36 bp deletion removes 12 amino acids from LTBP4's hinge region, resulting in increased release of latent TGFβ and increased TGFβ activity (7). Furthermore, single-nucleotide variants in human *LTBP4* associate with duration of ambulation in DMD boys, indicating LTBP4 modifies muscular dystrophy in both mice and humans (15,16). A second modifier was also discovered using QTL mapping in *Sgcg* mice. A cryptic splice variant in *Anxa6* was identified encoding a truncated annexin A6 protein that negatively modifies membrane repair (14).

We now examined QTL mapping data for body mass in the context of muscular dystrophy and identified an interval on chromosome 10 that contributes to body mass. We identified a variant in the dual-specificity phosphatase 6 (*Dusp6*) gene within this interval that correlated with body mass. The DUSP6 protein belongs to a family of mitogen-activated protein kinase (MAPK) phosphatases that specifically target and dephosphorylate MAPK/extracellular signal-regulated kinase (ERK) to negatively regulate this pathway (17–19). ERK activation associates with cell proliferation in multiple cell types including muscle (19–22). In this study, we show that a missense variant in *Dusp6* correlates with a partial loss of function of DUSP6 activity, thus promoting ERK activity. Furthermore, we show that treatment with a specific DUSP6 inhibitor leads to increased proliferation in myoblasts from the 129 but not D2 background. These findings identify DUSP6 as a target for regulating myoblast proliferation and muscle growth.

Results

Chromosomal loci associated with body mass in muscular dystrophy

The D2 mouse strain intensifies the phenotypes of muscular dystrophy compared with the 129 T2/SvEmsJ (129) mouse strain (6,10,11). To identify genetic regions influencing distinct properties related to muscular dystrophy, QTL mapping was carried out on a previously described F3 intercross of *Sgcg*-null mice from the D2 and 129 background strains (8). QTLRel was used to associate genetic intervals with total body mass from an F3 cohort of 189 mice (23). Two loci were identified with *P*-values ≤ 0.05. The first locus on chromosome 1 maps to an interval harboring the *Mstn* locus, which encodes myostatin, a profound regulator of body mass (24). A second locus on chromosome 10 was also found to be significantly associated with body mass (Fig. 1A). The 95% confidence interval for this region on chromosome 10 locus ranges from 40.67–54.96 cM (Fig. 1B and C).

Genetic background influences body and muscle mass

To evaluate whether strain differences modify mass, WT and *Sgcg*-null mice from the D2 and 129 strains were weighed and muscles were harvested at 14–15 weeks of age. For both WT male and females, D2 mice had significantly increased body mass compared with 129 mice. These findings are consistent with those reported on genetic background strains from the Jackson Laboratories (13). The increase in body mass conferred by the D2 strain was diminished in *Sgcg* muscular dystrophy mice indicating the dystrophic process itself alters body mass (Fig. 2A). Individual skeletal muscles were isolated and assessed for mass. In WT mice, females but not males exhibited increased muscle mass in D2 mice compared with 129 mice for the quadriceps and gastrocnemius muscle, illustrating that muscle is not the only determinant of the strain-dependent body mass differences in mouse strains. In muscular dystrophy models, the D2 strain exacerbates muscular dystrophy resulting in smaller muscles (6). Consistent with this prior observation, in the *Sgcg* muscular dystrophy muscle, the mass of individual muscles was significantly reduced by the D2 background compared with *Sgcg* mice in the 129 mice background strain (Fig. 2B and C). Similar to skeletal muscle, the heart showed strain-dependent differences in size. In the WT backgrounds, there was increased mass of the left ventricle (LV) and right ventricle (RV) in male D2 mice compared with male 129 mice ($P = 0.01$ and $P = 0.03$, respectively) (Supplementary Material, Fig. S1). Similar trends were seen for the LV in female mice, with D2 LV mass exceeding 129 LV mass ($P = 0.07$).

In skeletal muscle, we examined cross-sectional area (CSA) and fiber number as reflections of hypertrophy and hyperplasia, both of which contribute to mass. In WT quadriceps muscles, CSA was significantly increased ($P = 0.04$) in D2 compared with 129 but this difference was not seen in *Sgcg*-null dystrophic muscle from the two background strains. Fiber number was similar between WT D2 and WT 129 fast muscles, but *Sgcg*-null D2 quadriceps muscles had significantly reduced fiber number compared with *Sgcg*-null 129 ($P = 0.002$) (Supplementary Material, Figs S2A and S3A). We also evaluated the slow-twitch soleus muscle and found that CSA was similar between WT D2 and WT 129 soleus muscles, but in *Sgcg-null* dystrophic muscle,

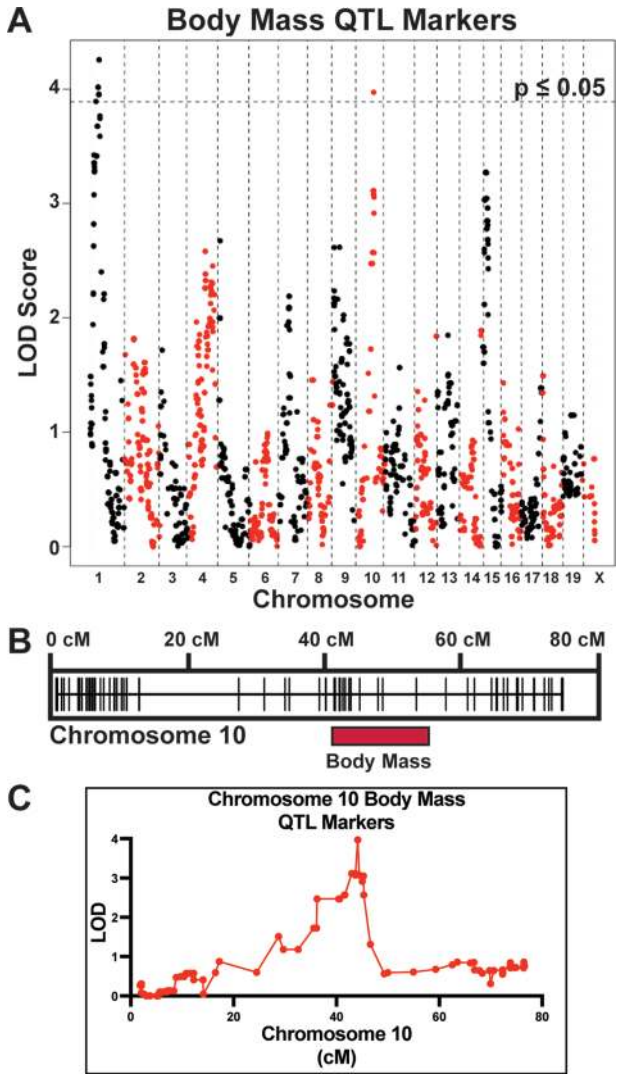

Figure 1. Chromosomal intervals contributing to body mass in muscular dystrophy identified by genome-wide mapping. QTL mapping was conducted using the *Sgcg* mouse muscular dystrophy model from the D2 and 129 strains. (**A**) The QTL plot for total body mass identified two loci that were significantly associated with total body mass on chromosome 1 ($P < 0.01$) and chromosome 10 ($P < 0.05$). (**B**) Genetic map of markers used for the QTL analysis on chromosome 10. The region associated with total body mass is from 40.67 to 54.96 cM on chromosome 10. (**C**) Single-QTL plot for chromosome 10 and markers associated with total body mass.

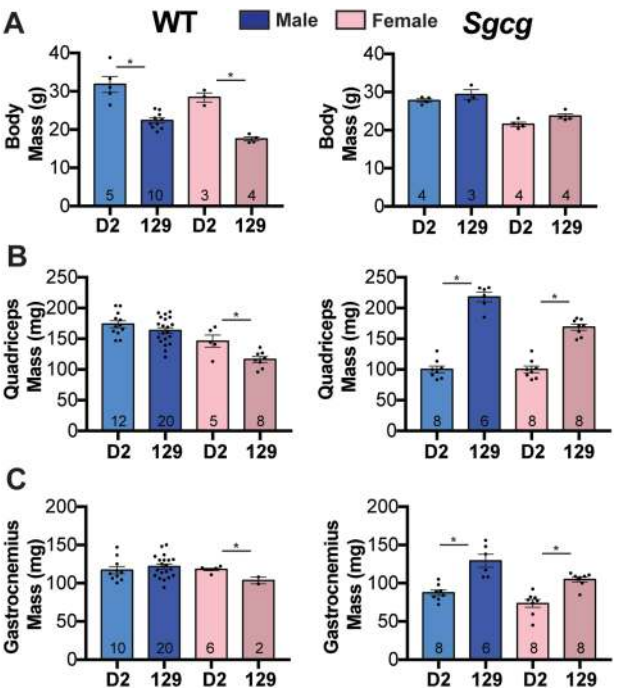

Figure 2. Genetic background influences body and muscle mass. WT (left) and *Sgcg*-null (right) mice were evaluated at 14–15 weeks of age. (**A**) Body mass was measured in D2 and 129 mice from WT and *Sgcg* animals. D2 mice have significantly increased body mass compared with 129 mice in the WT background but not in the *Sgcg*-null background (males, $P < 0.0001$; females, $P < 0.0002$). In WT mice, the quadriceps (**B**) and gastrocnemius (**C**) muscles were larger for female mice but not for males in the D2 compared with the 129 background strain ($P = 0.011$ female quadriceps and $P = 0.006$ female gastrocnemius). Conversely, muscle mass was significantly decreased in *Sgcg*-null D2 mice compared with *Sgcg*-null 129 mice for both quadriceps (males and females; $P < 0.0001$) and gastrocnemius (males $P = 0.0004$; females $P = 0.0002$). Comparisons by two-tailed student's *t*-test.

Sgcg-null D2 CSA was significantly smaller than *Sgcg*-null 129 ($P < 0.0001$). In soleus muscle, fiber number was increased in WT D2 compared with WT 129 ($P = 0.01$), and this difference was lost when comparing *Sgcg*-null D2 and *Sgcg*-null 129 soleus muscle fiber number (Supplementary Material, Figs S2B and S3B). Thus, the strain-dependent effects of background differ on fast and slow muscle, but muscular dystrophy is sufficient to override the genetic modifiers that normally make the D2 strain larger than the 129 strains.

Candidate modifier genes in the chromosome 10 interval

In order to identify candidate genetic modifiers of body mass, genomic differences between strains were identified and filtered in a step-wise manner using whole-genome sequence data comparing the parental D2 and 129 strains (8) (Supplementary Material, Fig. S4). Genomes from both the D2 and 129 strains were first aligned to the C57BL/6J (B6) mouse reference genome, version mm10 using the MegaSeq workflow and then compared (25). Protein-coding genes within the QTL interval were then assessed for nonsense and missense polymorphisms. Missense variations within canonical transcripts were further filtered and ranked based on whether they were predicted to be deleterious to protein function using the sorting intolerant from tolerant (SIFT) algorithm (26). RNA-sequencing data from muscle was used to compare expression difference. Variants were then validated using Sanger sequencing. The chromosome 10 QTL region contains a total of 136 protein-coding genes, 45 of which contained 172 missense and nonsense protein-coding variants when comparing between the D2 and 129 parental strains. Using SIFT to assess the potential effect on proteins, 11 missense variants were considered deleterious across six genes. Using RNA-seq, only three of these genes had relatively high expression in skeletal muscle, including *Dusp6* (Table 1).

DUSP6 as a candidate genetic modifier for body mass on chromosome 10

DUSP6 belongs to a family of phosphatases responsible for regulating the MAPK/ERK pathway (27,28). The MAPK/ERK

Table 1. Candidate modifiers genes for body mass based on coding region variation

Gene symbol	Gene name	Variant(s)	SIFT score	D2 expression CPM	129 expression CPM
Dusp6	DUSP6	rs13480726 (M62I)	0.01	55.3	24.5
Amdhd1	Amidohydrolase domain containing 1	rs29360688 (A391T)	0.01	<1	<1
Stab2	stabilin 2	rs29342083 (V1953A)	0.04	88.3	12.4
		rs29349759 (T1596M)	0.04		
		rs30241243 (P1086L)	0.01		
		rs48050828 (G864D)	0.01		
		rs235800634 (V302M)	0.03		
		rs30242264 (R151H)	0.01		
Usp44	ubiquitin specific peptidase 44	rs29335881 (H118Y)	0.01	<1	<1
Elk3	ELK3, member of ETS oncogene family	rs222449484 (A331T)	0.02	61.3	22.5
Ttc41	tetratricopeptide repeat domain 41	S480P	0.02	<1	<1

CPM, counts per million from RNA-seq.

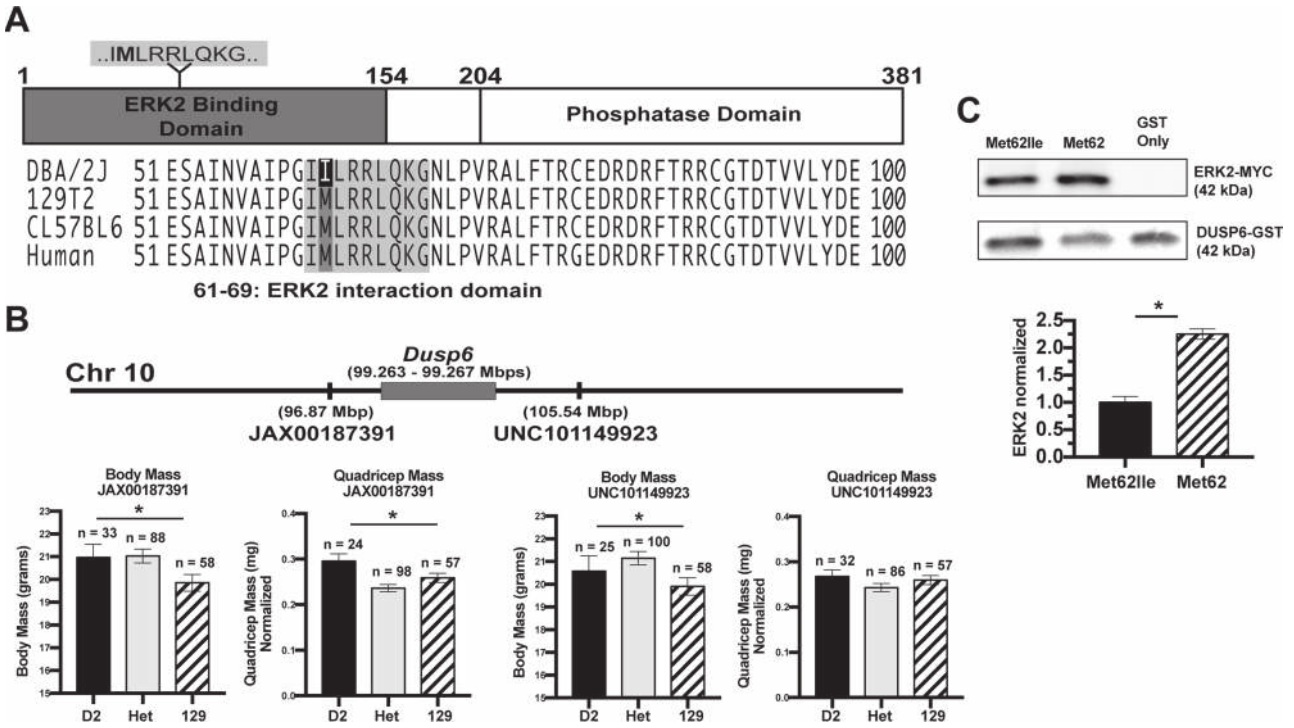

Figure 3. DUSP6 contains a Met62Ile substitution in the D2 strain that reduces ERK2 interaction. (**A**) The *Dusp6* Met62Ile variant (rs13480726) was identified in the D2 strain but not in other common mouse strains. Met62Ile is also conserved in human *DUSP6* and overall this domain, which mediates ERK binding, is highly conserved. (**B**) Genotypes of SNPs flanking the *Dusp6* region from a cohort of more than 175 intercross *Sgcg* F3 mice from a $Sgcg^{D2}$ X $Sgcg^{129}$ cross (14). SNPs flanking *DUSP6*, JAX00187391 and UNC101149923, from the F3 *Sgcg* intercross were analyzed for their association with body mass. Their relative position to *Dusp6* is shown on the top bar. Mice with the D2 genotype at both markers showed significant association with increased body mass ($P = 0.044$, $P = 0.042$). The most proximal marker to *Dusp6*, JAX00187391, showed a significant association between the D2 genotype and increased quadriceps muscle mass ($P = 0.003$). Comparisons by one-way ANOVA. (**C**) A GST-pulldown assay was performed to measure the interaction between ERK and DUSP6 using the ERK2 binding domain. DUSP6 Met62Ile displayed a significantly reduced interaction with ERK2 compared with DUSP6 Met62 ($P = 0.0009$, $n = 3$, two-tailed student's *t*-test.).

pathway is a central regulator of cell growth and differentiation and DUSPs regulate the MAPK pathway through their rapid dephosphorylation activity (19). DUSP6 is a highly specific negative regulator of this pathway through its dephosphorylation of ERK2 in the cytoplasm, which then inhibits translocation of ERK2 to the nucleus (29). We identified a *Dusp6* variant unique to the D2 strain, rs13480726, based on genome assembly GRCm38.p5 (Chromosome 10:99263877, c.186G > A, p.Met62Ile). The D2 strain has an isoleucine substituted for the methionine at position 62, and the D2 strain is the only mouse strain exhibiting this variant. The methionine at position 62 is highly conserved across species (Fig. 3A). Furthermore, this position falls directly within the ERK2- interaction domain that was previously mapped to amino acids 61–69 (30). Site directed mutagenesis of amino acids 63–65 was previously shown to result in loss of the direct interaction between DUSP6 and ERK2 (30). The loss of

DUSP6 binding by ERK2 had the net effect of increasing ERK2 activity (30).

We examined the genotypes of QTL single nucleotide polymorphism (SNP) markers, JAX00187391 and UNC101149923, as these flanked the *Dusp6* gene and were informative in the *Sgcg* F3 intercrossed cohort. *Sgcg* mice harboring the D2 SNPs in this chromosome 10 interval had increased body and quadriceps mass compared with the mice carrying SNPs derived from the 129 strains. Furthermore, the most proximal informative SNP to the *Dusp6* gene itself, JAX00187391, has the strongest association with increased mass compared with UNC101149923 (Fig. 3B). These data indicate that while overall, the D2 strain results in smaller muscles in muscular dystrophy mice, this effect is driven by other loci in the D2 genome. The genetic association data support that the *Dusp6* locus counteracts the overall D2 background effect and stimulates larger mass.

To test whether the Met62Ile substitution modified DUSP6's ability to interact with ERK2, we analyzed ERK2 binding with a mutated DUSP6 interaction domain (amino acids 1–154) using a Glutathione S-transferase (GST) pulldown assay. We found that substitution of Met62 with an isoleucine reduced binding by ~2-fold compared with the canonical DUSP6 interaction domain (Fig. 3C). We also evaluated the intracellular localization by transfecting GFP-tagged Met62Ile and Met62 DUSP6 into C2C12 cells. The Met62Ile substitution did not alter the cytoplasmic localization of DUSP6 nor its overall expression level indicative of similar protein stability when overexpressed in C2C12 cells (Supplementary Material, Fig. S5). Thus, the Met62Ile variant through a reduced ERK2 interaction is expected to enhance ERK2 phosphorylation and activity.

Increased phosphorylated ERK1/2 from the Met62Ile substitution in DUSP6

To assess the activity of DUSP6 harboring the Met62Ile substitution, we overexpressed DUSP6 with either methionine or isoleucine at position 62. Plasmids were introduced into C2C12 myoblasts and phosphorylation of ERK1/2 was monitored. A 50% increase in phosphorylated ERK1/2 (pERK) was seen in cells transfected with DUSP6 Met62Ile compared with cells transfected with DUSP6 Met62 (Fig. 4A). pERK levels were normalized to the amount of transfected DUSP6 in addition to input lanes to account for any differences in transfection efficiencies. No significant differences were observed for total ERK protein. Thus, the Met62Ile DUSP6 substitution showed a partial loss of function accounting for increased pERK and sustained pERK activity.

To assess whether pERK levels were changed *in vivo*, we assessed pERK levels in quadriceps muscles isolated from WT and muscular dystrophy mice from the D2 and 129 backgrounds. In the WT background, a trend toward increased pERK levels was seen for D2 mice (Fig. 4B, left). A 20% decrease in pERK levels was observed in *Sgcg* muscle from the D2 strain compared with *Sgcg* muscle from the 129 strains (Fig. 4B, right). No significant differences were observed for total ERK protein. To understand this result, we examined *Dusp6* gene expression in dystrophic muscle. RNA-sequencing data from WT and *Sgcg*-null quadriceps muscles was used to compare *Dusp6* gene expression from D2 and 129 mouse strains. We found that *Dusp6* transcript expression was significantly higher in D2 muscle compared with 129 in the WT backgrounds and that an even larger difference was seen in the *Sgcg*-null backgrounds (Fig. 4C). Immunoblotting was used to monitor DUSP6 protein in muscle. In the WT background, we detected similar amounts of DUSP6 protein between D2 and 129 muscles (Fig. 4D, left). However, the *Sgcg*-null muscle from the D2 background showed a 350% increase in DUSP6 protein (Fig. 4D, right). Together, these results indicate that while the Met62Ile substitution reduces DUSP6's binding by approximately half, in the setting of muscular dystrophy, the 350% upregulation of DUSP6 protein is sufficient to largely compensate for the partial loss of function.

Inhibition of DUSP6 results in increased myoblast proliferation

In muscle progenitor cells, ERK activation promotes cell proliferation (19). BCI (2-benzylidene-3-(cyclohexylamino)-1-Indanone hydrochloride), also known as NSC 150117, is a highly specific inhibitor of DUSP6 and was previously shown to prevent DUSP6-mediated pERK dephosphorylation by acting as an allosteric binding inhibitor in the phosphatase domain (31). We examined whether there was differential sensitivity to BCI between D2 and 129 myoblasts, as would be expected from the Met62Ile substitution in *Dusp6*. Myoblasts isolated from the D2 and 129 strains were treated with a range of concentrations of BCI (0, 0.5 and 2 μm) and then assessed for cell growth at multiple time points. Myoblasts from the 129 strains showed a dose-dependent increase in proliferation, consistent with the known activity of BCI, which by inhibiting DUSP6 activity promotes ERK activity (31). This effect was seen in myoblasts isolated from WT and *Sgcg* muscular dystrophy mice. In contrast, myoblasts from the D2 strain were resistant to BCI. At 0.5 μm and 2.0 μm BCI, myoblasts from the D2 strain showed little to no effect on myoblast growth from both WT and *Sgcg* mice (Fig. 5A and B). For both strains and genotypes, at higher concentrations of BCI (5.0 and 7.5 μm), myoblast proliferation was suppressed, suggestive of toxicity (Supplementary Material, Fig. S6). These data demonstrate a differential sensitivity to BCI where myoblasts from 129 strains respond to DUSP6 inhibition by BCI, whereas BCI has little effect on DUSP6 with the Met62Ile substitution, as this form already exhibits compromised function.

Discussion

MAPK/ERK as a modifier of mass

The MAPK/ERK pathway responds to a wide range of growth factors/mitogens and stress stimuli to send intracellular signals. Of the major MAPK pathways, the ERK1/2 pathway has been extensively linked to cell growth and proliferation through its role in regulating cell cycle progression. Once activated, ERK1/2 phosphorylates a wide range of intracellular substrates to regulate proliferation, differentiation and apoptosis (22). Studies in multiple different tissues such as skin, skeletal muscle and the heart have shown that loss of ERK1/2 signaling can inhibit proliferation. In myoblasts, fibroblast growth factor-stimulated ERK1/2 signaling is required for proliferation (32–34). Furthermore, ERK1/2 signaling has been shown to regulate hypertrophy in skeletal muscle (35). In mouse cardiac muscle, transgenic activation of ERK1/2 signaling promotes cardiac hypertrophy (36,37). In order to regulate both the magnitude and duration of these responses, MAPK phosphatases such as DUSP6 play a critical role by inactivating of ERK1/2 signaling, often with high specificity to more precisely regulate ERK signaling (30).

We now identified naturally occurring variation in the *Dusp6* gene in the DBA2J (D2) mouse genome as a modifier of body mass. This specific variant (Met62Ile) is only present in the D2 mouse strain and has not been reported in other mouse or human SNP databases. However, there is one heterozygous Met62Val allele of 238 244 alleles in the Genome Aggregation

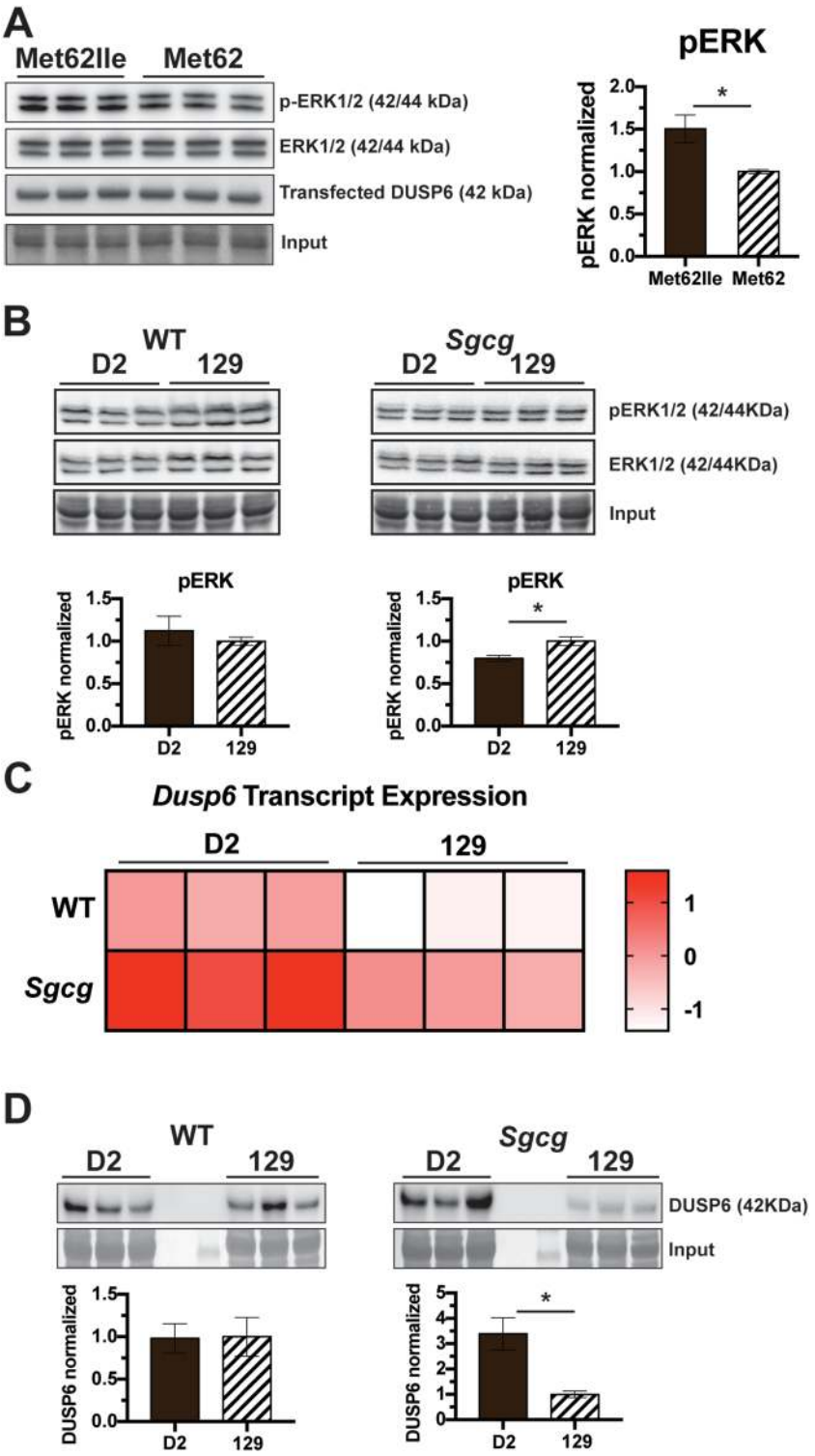

Figure 4. The DUSP6 Met62Ile substitution exhibits a partial loss of function as a regulator of ERK phosphorylation. (**A**) Immunoblotting was performed on C2C12 cell lysates to measure p-ERK levels following transfection of plasmids expressing DUSP6 Met62 or DUSP6 Met62Ile. Cells expressing DUSP6 Met62Ile exhibited significantly higher p-ERK levels compared with cells transfected with DUSP6 Met62 ($P = 0.04$, $n = 3$). (**B**) Immunoblotting was performed on protein lysates extracted from quadriceps muscle harvested from WT and *Sgcg* mice from the D2 and 129 backgrounds. $Sgcg^{129}$ mice showed significantly higher p-ERK levels compared with $Sgcg^{D2}$ mice ($P = 0.03$, $n = 3$). (**C**) RNA-seq analysis from WT and *Sgcg* quadriceps muscles revealed that expression of the *Dusp6* was significantly higher in the D2 strain than the 129 strains in both WT and *Sgcg* muscles ($P < 0.05$, $n = 3$). (**D**) Immunoblotting of quadriceps muscles showed significantly higher DUSP6 protein expression in the D2 strain from *Sgcg* muscle ($P = 0.03$, $n = 3$) but not WT muscle. Comparisons by two-tailed student's *t*-test.

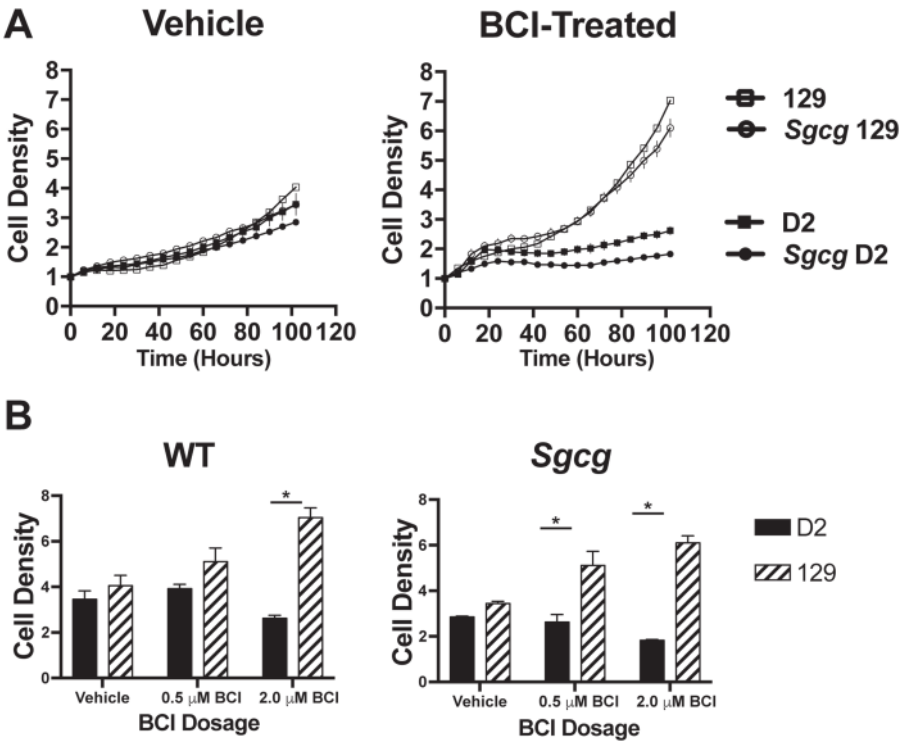

Figure 5. Myoblasts from the D2 background were insensitive to the DUSP6 inhibitor BCI. Myoblasts from D2 and 129 muscles were isolated, cultured and treated with the DUSP6-specific small molecule inhibitor BCI (also known as **NSC 150117**) (31). Myoblasts were treated with BCI at multiple concentrations, and proliferation was measured. **(A)** Myoblast growth curves from D2 and 129 WT and *Sgcg*-null mice treated with 0 μm BCI or 2.0 μm BCI. BCI treatment increased the proliferation of 129 myoblasts but had little to no effect on D2 myoblast proliferation. This increase in proliferation was seen for both myoblasts isolated from WT and *Sgcg*-null 129 mice. **(B)** Graphical representation of myoblast growth is shown measuring 4 days post-treatment and comparing D2 and 129 myoblasts treated with 0, 0.5 or 2.0 μm BCI. WT and *Sgcg*-null 129 myoblasts showed significantly increased growth from BCI treatment compared with WT and *Sgcg* D2 myoblasts. (*$P < 0.05$, by two-way ANOVA with Bonferonni correction).

Database (gnomAD) (MAF 4.197e-6). In humans, there are no loss of function variants in DUSP6 in the Exome Aggregation Consortium (ExAC) (constraint metric pLI = 0.91) and missense variants are lower than expected (constraint metric z = 2.72), indicating a comparatively low tolerance to variation. Although identified in the context of mouse muscular dystrophy, in principle, this effect should not be restricted to muscular dystrophy and may apply more broadly to tissue growth. We identified a missense variant that alters a methionine in the ERK binding domain of DUSP6. Prior studies implicated this same region as being essential to ERK binding and site directed mutagenesis in neighboring residues showed reduced interaction between DUSP6 and ERK (30). Perturbing DUSP6 binding to ERK was similarly associated with increased ERK phosphorylation and activity (30,38). Intriguingly, QTL mapping studies for mass, size and weight gain in pigs implicated a genomic locus that included porcine *DUSP6*, suggesting this pathway is active in other mammals beyond mice (39). Mice engineered to lack *Dusp6* had increased heart mass and fibroblasts and showed reduced apoptosis (40). In this model, *Dusp6*-null mice had improved cardiac compensation after myocardial injury (40). Furthermore, increased cardiomyocyte proliferation has been observed in *Dusp6*-null zebrafish as well as zebrafish treated with DUSP6 inhibitors (31,41). Together, these findings suggest a relationship between growth and DUSP6/ERK signaling in a number of cell types.

We found that the *Dusp6* genotype was associated with skeletal muscle mass, indicating that *Dusp6* likely regulates muscle mass in the same manner it can affect other cell types and tissues. We found that inhibition of DUSP6 activity increased proliferation of myoblasts from the 129 strains, which harbors a more canonical DUSP6 sequence. In contrast, the D2 strain, which carries the Met62Ile variant in DUSP6, failed to increase myoblast proliferation and was effectively resistant to inhibitors of DUSP6 activity. These data indicate that myoblasts are one cell type responsive to DUSP6 regulation of ERK1/2 and it is possible that both hyperplastic and hypertrophic mechanisms contribute to the effect of DUSP6 in muscle.

Is promoting mass in muscular dystrophy through ERK signaling beneficial?

It is widely believed that increasing muscle mass can benefit muscular dystrophy since increased mass is expected to convey increased strength. Loss of myostatin, the negative regulator of muscle mass improves muscle strength and reduces fibrosis in the *mdx* mouse model of Duchenne muscular (42). In humans, a previous clinical trial utilizing a myostatin antibody treatment shows trends of increased muscle mass and ambulation (43). Gene delivery of follistatin, a potent myostatin antagonist, also showed similar positive effects on muscle mass and ambulation (44). However, promoting muscle mass without sufficiently enhancing muscle regeneration in muscular dystrophy may also result in increased muscle damage due to excessive force production in an already weakened muscle. Specifically, in a canine model of DMD, myostatin inhibition led to unequal muscle growth and greater contractures (45). Muscle-specific

overexpression of follistatin in dysferlin-deficient mice exacerbated muscle degeneration (46). We now found that inhibition of DUSP6 promoted myoblast growth in genetically susceptible mice, but it remains to be seen whether this effect is helpful in a dystrophic context.

A complexity of the current study is that the effect on growth was more evident in WT animals than it was in muscular dystrophy animals, where much of the effect on growth was reversed presumably because of the influence of many other genomic loci in the DBA2J background, which overall inhibits muscle growth in muscular dystrophy (6). QTL mapping in mice has shown that growth in normal animals is under the influence of many different genomic intervals (47,48). Most QTL studies are conducted in WT mice, and the course of muscular dystrophy, with ongoing degeneration and regeneration, is a process that systemically activates many MAPK pathways. Consistent with the concept that DUSP6 itself is important for muscle function, and perhaps injury response, it has been shown that rapid upregulation of ERK1/2 signaling occurs in human skeletal muscle in response to exercise (49,50). Thus, the upregulation of ERK signaling occurs in normal muscle and mediates multiple responses after acute exercise. In dystrophic muscle, where there are many distinct cell types including myoblasts, fibroblasts, immune infiltrate cells and myofibers, ERK signaling may be more essential for some cell types compared with others. Taken together, these data show that a genetic variant associated with an ERK-modifying phosphatase differentially impacts myoblast proliferation and muscle growth in mice according to their genetic background, thus emphasizing the need to better decipher the genetic interactions instructing muscle homeostasis in normal and diseased conditions.

Materials and Methods

Ethics statement

Mice were housed and treated according to protocols approved by the Northwestern University's Institutional Animal Care and Use Committee. Mice were euthanized using carbon dioxide, cervical dislocation and removal of the heart. Methods were optimized for the reduction of pain and discomfort.

Mouse strains and QTL mapping

Sgcg mice were previously generated by deletion of exon 2 to create a null allele of *Sgcg* (9). *Sgcg* mice were then backcrossed into the DBA2J (D2) and 129 T2/SvEmsJ (129) backgrounds for more than 10 generations and then intercrossed to generated $Sgcg^{D2/129}$ animals (8). A previously described intercross was conducted between $Sgcg^{129}$ and $Sgcg^{D2}$ mice (14). Approximately 180 F3 intercrossed mice $Sgcg^{129/D2}$ were analyzed for body mass, muscle mass, fibrosis and Evans blue-dye uptake as described (8). QTL mapping was carried out using the Mouse Universal Genotyping Array and analyzed by QTLrel (23) to identify loci of interest. WT and *Sgcg* mice from the D2 or 129 backgrounds were analyzed and harvested at 14–15 weeks of age.

Whole-genome sequencing

Whole-genome sequencing of D2 and 129 mice was previously described (14). Genomes were now aligned to the mouse genome assembly mm10. Coding variants were assessed for predicted deleterious effect using the SIFT algorithm (26).

Plasmids

The plasmid encoding *Dusp6* was engineered with a carboxy-terminal Myc-DDK-tag (Origene Rockville, MD USA; Cat# MR222688). Site-directed mutagenesis was performed to create *Dusp6* variants. The DUSP6 interaction domain was amplified from resulting plasmids and cloned into a PGEX-4 T-3 GST vector (GE Life Sciences Marlborough, MA USA; Cat#28–9545-52). The *Mapk1* plasmid was engineered with a carboxy-terminal Myc-DDK-tag (Origene Rockville, MD USA; Cat# MR227633).

Cell isolation, culture and transfections

C2C12 cells (ATCC Manassas, VA USA; Cat# CRL-1772) were grown in Dulbecco's Modified Eagle Medium with 10% fetal bovine serum and 1% penicillin/streptomycin in 5% CO_2. Primary mouse myoblasts were isolated from hind limb muscles of 6- to 8-week-old mice using a previously described protocol (51). Myoblasts were grown in Ham's F-10 Nutrient Mixture (F-10) supplemented with 20% FBS, 2% penicillin/streptomycin and 10 ng/µl of fibroblast growth factor (Miltenyi Biotec Bergisch Gladbach, Germany Cat# 130–093-842) in 5% CO_2. C2C12 cells were plated at ∼70–80% confluency in a 60 mm dish with Opti-MEM Reduced Serum Media prior to transfection. Transfections used Lipofectamine 3000 Transfection Reagent (ThermoFisher Rockford, IL USA; Cat# L3000008). The p3000 reagent was used at a 2:1 P3000:DNA ratio to transfect 10 µg of desired plasmids into C2C12 cells. Cells were transfected overnight and replaced with growth media the following morning and were allowed to grow for 48 h prior to protein isolation.

BCI ((E)-2-benzylidene-3-(cyclohexylamino)-2,3-dihydro-1H-inden-1-one; 3-(cyclohexylamino)-2,3-dihydro-2-(phenylmethylene)-1Hinden-1-one; 2-benzylidene-3-(cyclohexylamino)-1-Indanone hydrochloride and also known as NSC 150117) was purchased as a lyophilized powder (Axon Med Reston, VA USA Cat#2178) and resuspended in DMSO. Approximately 3000 cells from each strain were plated in triplicates in 96 well plates and treated with BCI at varying concentrations (0, 0.5 and 2 µm) in 0.1% DMSO myoblast growth medium. Media was replaced with fresh media containing BCI every 48 h. Cells were imaged and analyzed for relative cell density at multiple time points using the IncuCyte plate imager.

Muscle fiber counts and cross-sectional analysis

Muscles were placed in 10% formaldehyde (ThermoFisher Rockford, IL USA; Cat#245–684) and embedded into paraffin. Sections from the center of the tissue were stained with hematoxylin and eosin (Newcomer Supply Middleton, WI USA; Cat#12013B; Cat#1070C). Whole muscle sections were imaged using an Axio Observer A1 microscope (Zeiss, Germany) using Zen software (Zeiss, Germany) with a 10× objective. Total muscle fiber counts were quantitated using FIJI (NIH Bethesda, MD USA). Fiber CSA was quantitated using FIJI (NIH Bethesda, MD USA) for quadriceps (vastus-intermedius) and soleus. $n \geq 3$ male mice per group.

Immunoblotting

Mice were euthanized at approximately 14–15 weeks of age. Quadriceps muscles were isolated and immediately placed in tissue lysis buffer (2 mM Ethylenediaminetetraacetic acid (EDTA), 50 mM HEPES pH 7.5, 150 mM NaCl, 10 mM NaF, 10 mM Na-pyrophosphate, 10% glycerol, 1% Triton X-100 and Roche cOmplete protease inhibitor). Tissue was homogenized using a

homogenizer (BioSpec Bartlesville, OK USA) and subsequently the Bio-Rad Bradford reagent was used to measure protein concentration. Tissue lysates were separated using a 4–15% Mini-PROTEAN pre-cast gel and transferred to a Polyvinylidene Difluoride Immobilon-P membrane (EMDMillipore Burlington, MA USA; Cat# IPVH00010). StartingBlock T20 TBS (ThermoFisher Rockford, IL USA; Cat# 37543) was used for blocking and incubation of antibodies. The anti-phosERK1/2 antibody was used at 1:2000 (Cell Signaling Danvers, MA USA; Cat#9101S). The anti-ERK1/2 antibody was used at 1:2000 (Cell Signaling Danvers, MA USA; Cat#9102S). The anti-DUSP6 antibody (Origene; Cat# TA301017) was used at 1:1000. The anti-Myc antibody was used at 1:1000 (Origene Rockville, MD USA; Cat#TA150014). The anti-GST antibody was used at 1:1000 (ThermoFisher Rockford, IL USA; Cat# MA4–004). Goat anti-mouse and anti-rabbit antibodies conjugated to horseradish peroxidase were used at 1:2000. Memcode membrane stain (ThermoFisher Rockford, IL USA; Cat# 24585) was used to detect total protein. The actin protein band at 43 KDa was used as the loading control. Image analysis was performed using ImageJ.

RNA-seq analysis

The Illumina TruSeq RNA Sample Prep Kit version 2.0 was used to generate RNA sequencing libraries from quadriceps muscles from three D2 and three 129 mice. The RNA samples were indexed with unique adapters and pooled for 100 bp paired-end sequencing using the Illumina HiSeq 2000. RNA-seq reads were aligned using TopHat v2.0.2 to the mouse genome assembly mm10. Transcripts were assessed and quantitated using HT-seq and analyzed for differential expression using EdgeR. Counts per million (CPM) were used to calculate differential expression. Heatmaps were made from Z-scores calculated from log transformed CPM values per gene.

Protein purification and GST pulldown

The PGEX-4 T-3 plasmid containing Met62 and Met62Ile DUSP6-GST was transformed into ROSETTA competent cells (EMDMillipore Burlington, MA USA; Cat# 70954–3). Bacteria was grown to an OD_{600} of 0.8 and then induced with 0.5 mM of IPTG for 2 h at 37° in a shaking incubator. DUSP6-GST protein was isolated using a GST spin purification kit (ThermoFisher Rockford, IL USA; Cat# 16107). ERK2 protein fused to a Myc tag was purchased from Origene (Rockville, MD USA; Cat# MR227633). Equal amounts of Met62 or Met62Ile DUSP6-GST were incubated with ERK2 and rotated overnight at 4°C in binding/washing buffer (50 mM Tris (pH 7.5), 0.1 mM EDTA, 1% Triton X-100, 10% glycerol, 1 mM PMSF and 1 mM DTT). To pull down GST, Glutathione agarose beads (ThermoFisher Rockford, IL USA; Cat# 16100) were added the next day and allowed to incubate for 2 h at 4°C and then washed with the washing buffer. Samples were eluted by incubation with Laemmli sample buffer (Biorad Hercules, CA USA; Cat# 161–0737) and boiling for 5 min. Samples were resolved by sodium dodecyl sulfate polyacrylamide gel electrophoresis (SDS-PAGE). Immunoblotting was done against Myc to detect ERK2-Myc and against GST to detect DUSP6-GST as a loading control.

Statistical analysis

GraphPad Prism was used and statistical tests were selected based on data distribution.

Supplementary Material

Supplementary Material is available at *HMG* online.

Conflict of Interest statement. The authors have no financial conflict of interest related to this work.

Funding

NIH (R01 HL061322 and U54 AR052646); Parent Project Muscular Dystrophy.

Author contributions

A.H.V. (conducted analysis, performed experiments, wrote manuscript); K.A.S. (QTL genotyping, phenotyping and analysis); A.W. (immunoblotting); Q.Q.G. (myoblast growth curves); A.R.D. (fiber-sizing analysis); K.S.F. (imaging); M.Q. (Myoblast isolation); M.H. (Mice breeding and maintenance); P.P.(Histology); Z.C., A.E., K.S. (RNA-seq, analysis, WGS); S.F.N. and E.M.M. (conceived experiments, reviewed data, edited manuscript).

References

1. Bonnemann, C.G., Modi, R., Noguchi, S., Mizuno, Y., Yoshida, M., Gussoni, E., McNally, E.M., Duggan, D.J., Angelini, C. and Hoffman, E.P. (1995) Beta-sarcoglycan (A3b) mutations cause autosomal recessive muscular dystrophy with loss of the sarcoglycan complex. *Nat. Genet.*, **11**, 266–273.
2. Nigro, V., de Sa Moreira, E., Piluso, G., Vainzof, M., Belsito, A., Politano, L., Puca, A.A., Passos-Bueno, M.R. and Zatz, M. (1996) Autosomal recessive limb-girdle muscular dystrophy, LGMD2F, is caused by a mutation in the delta-sarcoglycan gene. *Nat. Genet.*, **14**, 195–198.
3. Lamar, K.M. and McNally, E.M. (2014) Genetic modifiers for neuromuscular diseases. *J. Neuromuscul. Dis.*, **1**, 3–13.
4. Noguchi, S., McNally, E.M., Ben Othmane, K., Hagiwara, Y., Mizuno, Y., Yoshida, M., Yamamoto, H., Bonnemann, C.G., Gussoni, E., Denton, P.H. *et al.* (1995) Mutations in the dystrophin-associated protein gamma-sarcoglycan in chromosome 13 muscular dystrophy. *Science*, **270**, 819–822.
5. McNally, E.M., Passos-Bueno, M.R., Bonnemann, C.G., Vainzof, M., de Sa Moreira, E., Lidov, H.G., Othmane, K.B., Denton, P.H., Vance, J.M., Zatz, M. *et al.* (1996) Mild and severe muscular dystrophy caused by a single gamma-sarcoglycan mutation. *Am. J. Hum. Genet.*, **59**, 1040–1047.
6. Heydemann, A., Huber, J.M., Demonbreun, A., Hadhazy, M. and McNally, E.M. (2005) Genetic background influences muscular dystrophy. *Neuromuscul. Disord.*, **15**, 601–609.
7. Heydemann, A., Ceco, E., Lim, J.E., Hadhazy, M., Ryder, P., Moran, J.L., Beier, D.R., Palmer, A.A. and McNally, E.M. (2009) Latent TGF-beta-binding protein 4 modifies muscular dystrophy in mice. *J. Clin. Invest.*, **119**, 3703–3712.
8. Swaggart, K.A., Heydemann, A., Palmer, A.A. and McNally, E.M. (2011) Distinct genetic regions modify specific muscle groups in muscular dystrophy. *Physiol. Genomics*, **43**, 24–31.
9. Hack, A.A., Ly, C.T., Jiang, F., Clendenin, C.J., Sigrist, K.S., Wollmann, R.L. and McNally, E.M. (1998) Gamma-sarcoglycan deficiency leads to muscle membrane defects and apoptosis independent of dystrophin. *J. Cell. Biol.*, **142**, 1279–1287.
10. Fukada, S., Morikawa, D., Yamamoto, Y., Yoshida, T., Sumie, N., Yamaguchi, M., Ito, T., Miyagoe-Suzuki, Y., Takeda, S.,

Tsujikawa, K. *et al.* (2010) Genetic background affects properties of satellite cells and mdx phenotypes. *Am. J. Pathol.*, **176**, 2414–2424.
11. Coley, W.D., Bogdanik, L., Vila, M.C., Yu, Q., Van Der Meulen, J.H., Rayavarapu, S., Novak, J.S., Nearing, M., Quinn, J.L., Saunders, A. *et al.* (2016) Effect of genetic background on the dystrophic phenotype in mdx mice. *Hum. Mol. Gen.*, **25**, 130–145.
12. Straub, V., Rafael, J.A., Chamberlain, J.S. and Campbell, K.P. (1997) Animal models for muscular dystrophy show different patterns of sarcolemmal disruption. *J. Cell. Biol.*, **139**, 375–385.
13. Bogue, M.A., Grubb, S.C., Walton, D.O., Philip, V.M., Kolishovski, G., Stearns, T., Dunn, M.H., Skelly, D.A., Kadakkuzha, B., TeHennepe, G. *et al.* (2018) Mouse Phenome Database: an integrative database and analysis suite for curated empirical phenotype data from laboratory mice. *Nucleic Acids Res.*, **46**, D843–D850.
14. Swaggart, K.A., Demonbreun, A.R., Vo, A.H., Swanson, K.E., Kim, E.Y., Fahrenbach, J.P., Holley-Cuthrell, J., Eskin, A., Chen, Z., Squire, K. *et al.* (2014) Annexin A6 modifies muscular dystrophy by mediating sarcolemmal repair. *Proc. Natl. Acad. Sci. U. S. A.*, **111**, 6004–6009.
15. Flanigan, K.M., Ceco, E., Lamar, K.M., Kaminoh, Y., Dunn, D.M., Mendell, J.R., King, W.M., Pestronk, A., Florence, J.M., Mathews, K.D. *et al.* (2013) LTBP4 genotype predicts age of ambulatory loss in Duchenne muscular dystrophy. *Ann. Neurol.*, **73**, 481–488.
16. van den Bergen, J.C., Hiller, M., Bohringer, S., Vijfhuizen, L., Ginjaar, H.B., Chaouch, A., Bushby, K., Straub, V., Scoto, M., Cirak, S. *et al.* (2014) Validation of genetic modifiers for Duchenne muscular dystrophy: a multicentre study assessing SPP1 and LTBP4 variants. *J. Neurol. Neurosurg. Psychiatry*, **86**, 1060–1065.
17. Mebratu, Y. and Tesfaigzi, Y. (2009) How ERK1/2 activation controls cell proliferation and cell death: is subcellular localization the answer? *Cell Cycle*, **8**, 1168–1175.
18. Shaul, Y.D. and Seger, R. (2007) The MEK/ERK cascade: from signaling specificity to diverse functions. *Biochim. Biophys. Acta*, **1773**, 1213–1226.
19. Michailovici, I., Harrington, H.A., Azogui, H.H., Yahalom-Ronen, Y., Plotnikov, A., Ching, S., Stumpf, M.P., Klein, O.D., Seger, R. and Tzahor, E. (2014) Nuclear to cytoplasmic shuttling of ERK promotes differentiation of muscle stem/progenitor cells. *Development*, **141**, 2611–2620.
20. Lawan, A., Min, K., Zhang, L., Canfran-Duque, A., Jurczak, M.J., Camporez, J.P.G., Nie, Y., Gavin, T.P., Shulman, G.I., Hernandez-Fernando, C. *et al.* (2018) Skeletal muscle-specific deletion of MKP-1 reveals a p38 MAPK/JNK/Akt signaling node that regulates obesity-induced insulin resistance. *Diabetes*, **67**, 624–635.
21. Wales, S., Hashemi, S., Blais, A. and McDermott, J.C. (2014) Global MEF2 target gene analysis in cardiac and skeletal muscle reveals novel regulation of DUSP6 by p38MAPK-MEF2 signaling. *Nucleic Acids Res.*, **42**, 11349–11362.
22. Meloche, S. and Pouyssegur, J. (2007) The ERK1/2 mitogen-activated protein kinase pathway as a master regulator of the G1- to S-phase transition. *Oncogene*, **26**, 3227–3239.
23. Cheng, R., Abney, M., Palmer, A.A. and Skol, A.D. (2011) QTLRel: an R package for genome-wide association studies in which relatedness is a concern. *BMC Genet.*, **12**, 66.
24. McPherron, A.C., Lawler, A.M. and Lee, S.J. (1997) Regulation of skeletal muscle mass in mice by a new TGF-beta superfamily member. *Nature*, **387**, 83–90.
25. Puckelwartz, M.J., Pesce, L.L., Nelakuditi, V., Dellefave-Castillo, L., Golbus, J.R., Day, S.M., Cappola, T.P., Dorn, G.W. 2nd, Foster, I.T. and McNally, E.M. (2014) Supercomputing for the parallelization of whole genome analysis. *Bioinformatics*, **30**, 1508–1513.
26. Kumar, P., Henikoff, S. and Ng, P.C. (2009) Predicting the effects of coding non-synonymous variants on protein function using the SIFT algorithm. *Nat. Protoc.*, **4**, 1073–1081.
27. Kondoh, K. and Nishida, E. (2007) Regulation of MAP kinases by MAP kinase phosphatases. *Biochim. Biophys. Acta*, **1773**, 1227–1237.
28. Li, C., Scott, D.A., Hatch, E., Tian, X. and Mansour, S.L. (2007) Dusp6 (Mkp3) is a negative feedback regulator of FGF-stimulated ERK signaling during mouse development. *Development*, **134**, 167–176.
29. Arkell, R.S., Dickinson, R.J., Squires, M., Hayat, S., Keyse, S.M. and Cook, S.J. (2008) DUSP6/MKP-3 inactivates ERK1/2 but fails to bind and inactivate ERK5. *Cell. Signal.*, **20**, 836–843.
30. Farooq, A., Chaturvedi, G., Mujtaba, S., Plotnikova, O., Zeng, L., Dhalluin, C., Ashton, R. and Zhou, M.M. (2001) Solution structure of ERK2 binding domain of MAPK phosphatase MKP-3: structural insights into MKP-3 activation by ERK2. *Mol. Cell.*, **7**, 387–399.
31. Molina, G., Vogt, A., Bakan, A., Dai, W., Queiroz de Oliveira, P., Znosko, W., Smithgall, T.E., Bahar, I., Lazo, J.S., Day, B.W. *et al.* (2009) Zebrafish chemical screening reveals an inhibitor of Dusp6 that expands cardiac cell lineages. *Nat. Chem. Biol.*, **5**, 680–687.
32. Lefloch, R., Pouyssegur, J. and Lenormand, P. (2008) Single and combined silencing of ERK1 and ERK2 reveals their positive contribution to growth signaling depending on their expression levels. *Mol. Cell. Biol.*, **28**, 511–527.
33. Scholl, F.A., Dumesic, P.A., Barragan, D.I., Harada, K., Bissonauth, V., Charron, J. and Khavari, P.A. (2007) Mek1/2 MAPK kinases are essential for Mammalian development, homeostasis, and Raf-induced hyperplasia. *Dev. Cell*, **12**, 615–629.
34. Jones, N.C., Fedorov, Y.V., Rosenthal, R.S. and Olwin, B.B. (2001) ERK1/2 is required for myoblast proliferation but is dispensable for muscle gene expression and cell fusion. *J. Cell. Physiol.*, **186**, 104–115.
35. Shi, H., Zeng, C., Ricome, A., Hannon, K.M., Grant, A.L. and Gerrard, D.E. (2007) Extracellular signal-regulated kinase pathway is differentially involved in beta-agonist-induced hypertrophy in slow and fast muscles. *Am. J. Physiol. Cell. Physiol.*, **292**, C1681–C1689.
36. Bueno, O.F. and Molkentin, J.D. (2002) Involvement of extracellular signal-regulated kinases 1/2 in cardiac hypertrophy and cell death. *Circ. Res.*, **91**, 776–781.
37. Bueno, O.F., De Windt, L.J., Tymitz, K.M., Witt, S.A., Kimball, T.R., Klevitsky, R., Hewett, T.E., Jones, S.P., Lefer, D.J., Peng, C.F. *et al.* (2000) The MEK1-ERK1/2 signaling pathway promotes compensated cardiac hypertrophy in transgenic mice. *EMBO J.*, **19**, 6341–6350.
38. Zhou, B., Zhang, J., Liu, S., Reddy, S., Wang, F. and Zhang, Z.Y. (2006) Mapping ERK2-MKP3 binding interfaces by hydrogen/deuterium exchange mass spectrometry. *J. Biol. Chem.*, **281**, 38834–38844.
39. Ramos, A.M., Pita, R.H., Malek, M., Lopes, P.S., Guimaraes, S.E. and Rothschild, M.F. (2009) Analysis of the mouse high-growth region in pigs. *J. Anim. Breed. Genet.*, **126**, 404–412.
40. Maillet, M., Purcell, N.H., Sargent, M.A., York, A.J., Bueno, O.F. and Molkentin, J.D. (2008) DUSP6 (MKP3) null mice show

enhanced ERK1/2 phosphorylation at baseline and increased myocyte proliferation in the heart affecting disease susceptibility. *J. Biol. Chem.*, **283**, 31246–31255.
41. Missinato, M.A., Saydmohammed, M., Zuppo, D.A., Rao, K.S., Opie, G.W., Kuhn, B. and Tsang, M. (2018) Dusp6 attenuates Ras/MAPK signaling to limit zebrafish heart regeneration. *Development*, **145**, 5.
42. Wagner, K.R., McPherron, A.C., Winik, N. and Lee, S.J. (2002) Loss of myostatin attenuates severity of muscular dystrophy in mdx mice. *Ann. Neurol.*, **52**, 832–836.
43. Campbell, C., McMillan, H.J., Mah, J.K., Tarnopolsky, M., Selby, K., McClure, T., Wilson, D.M., Sherman, M.L., Escolar, D. and Attie, K.M. (2017) Myostatin inhibitor ACE-031 treatment of ambulatory boys with Duchenne muscular dystrophy: results of a randomized, placebo-controlled clinical trial. *Muscle Nerve*, **55**, 458–464.
44. Mendell, J.R., Sahenk, Z., Al-Zaidy, S., Rodino-Klapac, L.R., Lowes, L.P., Alfano, L.N., Berry, K., Miller, N., Yalvac, M., Dvorchik, I. *et al.* (2017) Follistatin gene therapy for sporadic inclusion body myositis improves functional outcomes. *Mol. Ther.*, **25**, 870–879.
45. Kornegay, J.N., Bogan, D.J., Bogan, J.R., Dow, J.L., Wang, J., Fan, Z., Liu, N., Warsing, L.C., Grange, R.W., Ahn, M. *et al.* (2016) Dystrophin-deficient dogs with reduced myostatin have unequal muscle growth and greater joint contractures. *Skelet. Muscle*, **6**, 14.
46. Lee, Y.S., Lehar, A., Sebald, S., Liu, M., Swaggart, K.A., Talbot, C.C. Jr., Pytel, P., Barton, E.R., McNally, E.M. and Lee, S.J. (2015) Muscle hypertrophy induced by myostatin inhibition accelerates degeneration in dysferlinopathy. *Hum. Mol. Genet.*, **24**, 5711–5719.
47. Brockmann, G.A., Kratzsch, J., Haley, C.S., Renne, U., Schwerin, M. and Karle, S. (2000) Single QTL effects, epistasis, and pleiotropy account for two-thirds of the phenotypic f(2) variance of growth and obesity in DU6i × DBA/2 mice. *Genome Res.*, **10**, 1941–1957.
48. Suto, J.I. and Kojima, M. (2017) Quantitative trait loci that control body weight in DDD/Sgn and C57BL/6J inbred mice. *Mamm. Genome*, **28**, 13–19.
49. Krook, A., Widegren, U., Jiang, X.J., Henriksson, J., Wallberg-Henriksson, H., Alessi, D. and Zierath, J.R. (2000) Effects of exercise on mitogen- and stress-activated kinase signal transduction in human skeletal muscle. *Am. J. Physiol. Regul. Integr. Comp. Physiol.*, **279**, R1716–R1721.
50. Widegren, U., Ryder, J.W. and Zierath, J.R. (2001) Mitogen-activated protein kinase signal transduction in skeletal muscle: effects of exercise and muscle contraction. *Acta Physiol. Scand.*, **172**, 227–238.
51. Hindi, L., McMillan, J.D., Afroze, D., Hindi, S.M. and Kumar, A. (2017) Isolation, culturing, and differentiation of primary myoblasts from skeletal muscle of adult mice. *Bio. Protoc.*, **7**, 9.